
**Liquid Crystals**
Publication details, including instructions for authors and subscription information:
http://www.informaworld.com/smpp/title~content=t713926090

# Crystal-smectic E mesophases in a series of 2-(4-*n*-alkylphenyl)indenes

Steven M. Schultz[a]; Gerald Kehr[a]; Roland Fröhlich[a]; Gerhard Erker[a]; Nadia Kapernaum[b]; Constanze Hägele[b]; Frank Giesselmann[b]; Sabine Laschat[c]; Roxana Judele[c]; Angelika Baro[c]
[a] Organisch Chemisches Institut der Universität Münster, D-48149 Münster, Germany [b] Institut für Physikalische Chemie, Universität Stuttgart, D-70569 Stuttgart, Germany [c] Institut für Organische Chemie, Universität Stuttgart, D-70569 Stuttgart, Germany

**To cite this Article** Schultz, Steven M. , Kehr, Gerald , Fröhlich, Roland , Erker, Gerhard , Kapernaum, Nadia , Hägele, Constanze , Giesselmann, Frank , Laschat, Sabine , Judele, Roxana and Baro, Angelika(2007) 'Crystal-smectic E mesophases in a series of 2-(4-*n*-alkylphenyl)indenes', Liquid Crystals, 34: 8, 919 — 926
**To link to this Article: DOI:** 10.1080/02678290701541504
**URL:** http://dx.doi.org/10.1080/02678290701541504

*Liquid Crystals*, Vol. 34, No. 8, August 2007, 919–926

Taylor & Francis
Taylor & Francis Group

# Crystal-smectic E mesophases in a series of 2-(4-*n*-alkylphenyl)indenes

STEVEN M. SCHULTZ†, GERALD KEHR†, ROLAND FRÖHLICH†, GERHARD ERKER†, NADIA KAPERNAUM‡, CONSTANZE HÄGELE‡, FRANK GIESSELMANN‡, SABINE LASCHAT*§, ROXANA JUDELE§ and ANGELIKA BARO§

†Organisch Chemisches Institut der Universität Münster, Corrensstr. 40, D-48149 Münster, Germany
‡Institut für Physikalische Chemie, Universität Stuttgart, Pfaffenwaldring 55, D-70569 Stuttgart, Germany
§Institut für Organische Chemie, Universität Stuttgart, Pfaffenwaldring 55, D-70569 Stuttgart, Germany

(*Received 10 November 2006; in final form 9 May 2007; accepted 14 June 2007*)

A series of 2-(4-*n*-alkylphenyl)indenes (**3**) with different alkyl substituents ($CH_3$ to $C_{10}H_{21}$) were synthesized and systematically characterized using differential scanning calorimetry, polarizing optical microscopy and X-ray diffraction compared with 2-phenylindene (**3a**). Depending on the alkyl chain length, highly ordered crystal-smectic E mesophases were observed and confirmed by X-ray diffraction for the derivatives **3h–3k** with heptyl to decyl chains ($n=6-9$). For **3f** with a pentyl side chain ($n=4$), an X-ray crystal structure analysis was carried out.



## 1. Introduction

Looking at any classical textbook on liquid crystals [1], the typical structure of calamitic mesogenic molecules consists of an elongated stiff core unit substituted at the ends by long flexible alkyl chains or at least one alkyl chain and a polar head group (e.g. cyano) (figure 1).

Exceptions from this general pattern, where one substituent is missing (figure 1c), are rarely described. To the best of our knowledge so far only two mesogens possessing one flexible tail and no other substituent on the opposite side have been reported for liquid crystalline phases, namely isobutyl 4-(4′-phenylbenzylideneamino)cinnamate (**1**) [2] and 6-octyl-2-phenylazulene (**2**) [3] (scheme 1). Most interestingly, both compounds exhibit the quite rare crystal-smectic E phase only. In a patent [4], the application of 2-arylindene-based mesogens **3** (scheme 1) as components of liquid crystal media for electrooptical displays was envisaged. However, with the exception of the propyl-substituted phenylindene ($n=2$), the preparation of homologues and investigations concerning mesophases and their characterization are missing. Compounds **3** have been previously used only in Ziegler–Natta catalysis [5]. Furthermore, the number of compounds exhibiting the direct crystal-smectic E to isotropic liquid transition is very few [6]. In this paper, we report the synthesis and characterization of a series of derivatives (**3**) bearing alkyl chains of various lengths at one end. Furthermore, it seemed attractive to explore for the first time in more detail this aryl–aryl–alkyl side chain motif with respect to phase transition temperatures and packing behaviour in the mesophase. The results towards this goal are discussed below.

## 2. Experimental

### 2.1. *Characterization*

Differential scanning calorimetry (DSC) was performed using a Mettler Toledo DSC822 and polarizing optical

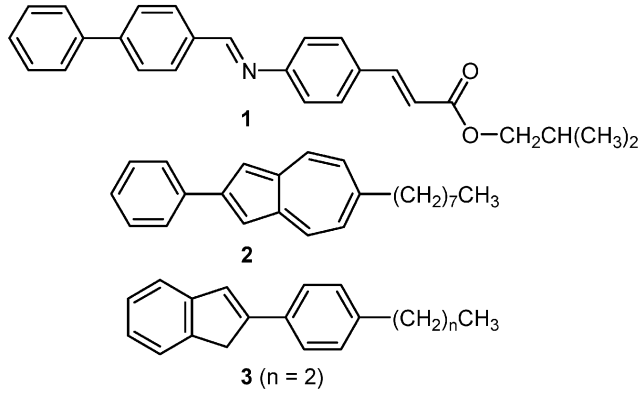


Scheme 1. Non-conventional mesogenic molecules with only one lateral alkyl side chain [2–4].

*Corresponding author. Email: sabine.laschat@oc.uni-stuttgart.de

*Liquid Crystals*
ISSN 0267-8292 print/ISSN 1366-5855 online © 2007 Taylor & Francis
http://www.tandf.co.uk/journals
DOI: 10.1080/02678290701541504

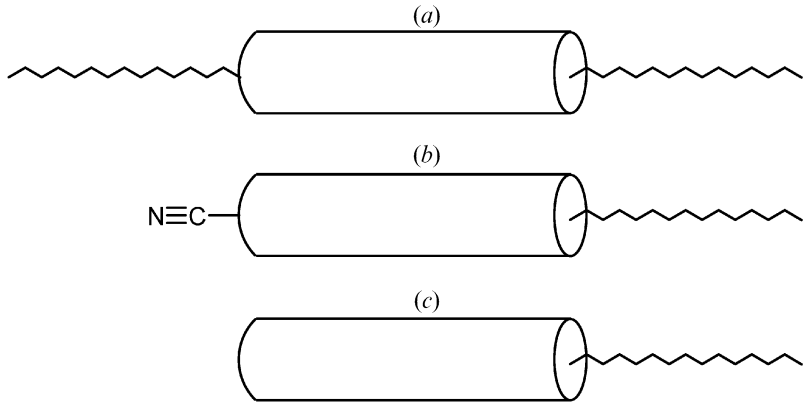


Figure 1. Schematic illustration of possible structures of conventional (a, b) and non-conventional calamitic mesogenic molecules (c).



microscopy (POM) using an Olympus BH-2, Leica DM-LP polarizing microscope combined with a Mettler FP 5 hot stage and Instec HS1-i central processor. X-ray experiments were performed with Ni-filtered Cu $K_\alpha$ radiation (wavelength 1.5418 Å). Small-angle scattering data from unaligned samples (filled into Mark capillary tubes of 0.7 mm diameter) were obtained using a Kratky compact camera (A. Paar) equipped with a temperature controller (A. Paar) and a one-dimensional electronic detector (M. Braun). Aligned samples were exposed in a home-made flat film camera and the two-dimensional (2D) diffraction patterns recorded with an imaging plate detector (Fuji BAS SR). In the flat film camera, the sample was placed in a small hole of a brass block, whose temperature was controlled by a Lakeshore controller and kept in a 1.5 T magnetic field for alignment.

## 2.2. *Syntheses*

**2.2.1. 4-(2-Alkenyl)bromobenzenes (5).** A 1.6 M solution of *n*-BuLi in hexane (20 ml, 32 mmol) was added via syringe to a suspension of **4g–4k** (32 mmol) and THF (250 ml) at 0°C in a 500 ml round-bottom flask. The red reaction mixture was stirred for 2 h. A solution of 4-bromobenzaldehyde (5.89 g, 36.6 mmol) in THF (100 ml) was added and the reaction mixture stirred overnight. The resulting suspension was washed with brine (3 × 50 ml). THF was removed under reduced pressure and the product was extracted from solid triphenylphosphine oxide with heptane. After removal of heptane, the crude product was filtered through a small silica gel plug (3 cm × 10 cm) with heptane to yield pure **5g–5k** as colourless oils.

**2.2.2. 4-*n*-Alkylbromobenzenes (6).** A Schlenk flask was charged with EtOH (100 ml) and Wilkinson's catalyst [$RhCl(PPh_3)_3$, 200 mg, 0.22 mmol]. Hydrogenation of **5g–5k** (267 mmol) for three days under $H_2$ (0.5 bar) yielded, after removal of EtOH and filtration through silica gel with heptane, **6g–6k** as colourless oils.

**2.2.3. 2-(4-*n*-Alkylphenyl)indenes (3).** The Grignard reagents were prepared from Mg turnings (29 mmol) and **6b–6k** (27 mmol) in THF. The Kumada coupling was carried out by adding the respective Grignard solution dropwise to a THF solution of 2-bromoindene (27 mmol) and $NiCl_2$(dppe) (180 mg, 0.34 mmol). The exothermic reactions were allowed to cool to room temperature and stirred for a further 2 h. After removal of the solvent and filtration through silica gel with heptane, the products (**3b–3k**) were isolated as white solids. Representative characterization data are given for **3b** and **3f**.

For **3b** [7], $^1$H NMR (500 MHz, $CD_2Cl_2$): 7.55 (m, 2H, Ph–H); 7.48 (m, 1H, Ph–H); 7.39 (m, 1H, Ph–H); 7.27 (m, 1H, Ph–H); 7.21 (m, 2H, Ph–H); 7.20 (m, 1H, Ph–H); 7.17 (m, 1H, Ph–H); 3.79 (bs, 2H, $CH_2$); 2.38 (m, 3H, $CH_3$). $^{13}$C NMR (125 MHz, $CD_2Cl_2$): 147.2, 146.1, 143.7, 138.1 (Ph); 133.7 (C); 129.9, 127.1, 126.1 (Ph); 126.0 (CH); 125.1, 124.1, 121.3 (Ph); 39.6 ($CH_2$); 21.5 ($CH_3$). GC-MS (EI 70 eV) *m*/*z* (%)=206 (100) [$M^+$], 191 (70).

For **3f**, $^1$H NMR (600 MHz, $CD_2Cl_2$): 7.57 (m, 2H, Ph–H); 7.47 (m, 1H, Ph–H); 7.34 (m, 1H, Ph–H); 7.25 (m, 1H, Ph–H); 7.21 (m, 2H, Ph–H); 7.20 (m, 1H, CH); 7.16 (m, 1H, Ph–H); 3.79 (bs, 2H, $CH_2$); 2.62 (m, 2H, $CH_2$); 1.63 (m, 2H, $CH_2$); 1.35 (m, 4H, $CH_2$); 0.91 (t, 3H, $CH_3$). $^{13}$C NMR (150 MHz, $CD_2Cl_2$): 146.6, 145.5, 143.1, 142.7 (Ph); 133.3 (C); 128.7, 126.5, 125.5 (Ph); 125.4 (CH); 124.5, 123.5, 120.6 (Ph); 39.0, 35.6, 31.5, 31.1, 22.5 ($CH_2$); 13.8 ($CH_3$). GC-MS (EI 70 eV) *m*/*z* (%)=262 (95) [$M^+$], 205 (100). Elemental analysis:

calculated for $C_{20}H_{22}$, C 91.55, H 8.45; found, C 91.43, H 8.34%.

## 3. Results and discussion

As shown in scheme 2, 4-alkylbromobenzenes (**6g–6k**) [8] with longer alkyl chains, which are not commercially available, were prepared by Wittig olefination [9] of the corresponding phosphonium salts (**4g–4k**) with 4-bromobenzaldehyde to give the olefinic coupling products **5g–5k** in 63–88% yield.

Subsequent selective catalytic hydrogenation with about 0.5 mol. % of Wilkinson's catalyst in ethanol at 0.5 bar $H_2$ for three days at ambient temperature afforded the 4-alkylbromobenzenes (**6g–6k**) in excellent yields of 93–98%. This specific hydrogenation protocol was necessary to avoid hydrogenolytic cleavage of the Br–C($sp^2$) bond which takes place under more forcing conditions. The target 2-(4-alkylphenyl)indenes (**3b–3k**) were obtained in 37–86% yield by nickel-catalyzed Kumada cross-coupling reaction [10] of **6b–6k** with 2-bromoindene [11].

2-(4-*n*-Pentylphenyl)indene (**3f**) was characterized by X-ray crystal structure analysis (figure 2a) [12]. The molecules of **3f** feature a planar carbon framework with a maximally extended pentyl chain.

The crystal packing diagram (figure 2b) shows that the individual molecules of **3f** in the crystal are arranged with their major vectors oriented parallel, forming a loose layered structure similar to that which may be present in the smectic mesogenic phase that is formed from this and its related systems (see below).

The mesomorphic properties of compounds **3b–3k** were investigated by DSC, POM and X-ray diffraction experiments in comparison with 2-phenylindene (**3a**). The results of the DSC experiments are summarized in table 1. The parent compound (**3a**) and the methyl- and ethyl-substituted derivatives (**3b** and **3c**) were non-mesogenic and displayed isotropic melting during heating and cooling cycles. 2-(4-*n*-Butylphenyl)indene (**3e**) was also non-mesogenic; however, it showed an additional crystal to crystal transition during the first heating. Surprisingly, the propyl derivative (**3d**) turned out to be mesogenic, as supported by POM observations. Upon heating or cooling mosaic textures were observed under the microscope. 2-(4-*n*-Alkylphenyl)indenes (**3f–3k**) with longer alkyl chain ($C_5H_{11}$ to $C_{10}H_{21}$) displayed a melting transition and a clearing transition during both heating and cooling cycles in DSC studies. In addition, pentyl- (**3f**) and octyl-substituted phenylindene (**3i**) displayed crystal to crystal transitions upon first heating, whereas 2-(4-*n*-decylphenyl)indene (**3k**) showed perfect enantiotropic behaviour, i.e. crystal to crystal, crystal to mesophase and mesophase to isotropic transitions were visible both in the heating and cooling cycles (table 1). Figure 3 shows the corresponding DSC curves of homologue **3k**.

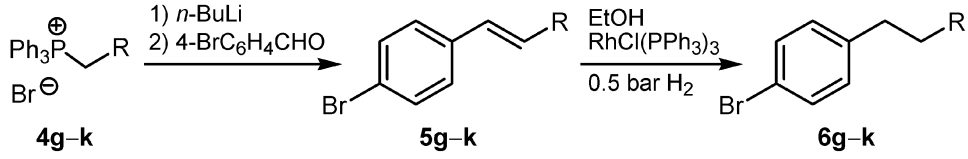


| 4–6 | g | h | i | j | k |
|---|---|---|---|---|---|
| R | $C_4H_9$ | $C_5H_{11}$ | $C_6H_{13}$ | $C_7H_{15}$ | $C_8H_{17}$ |

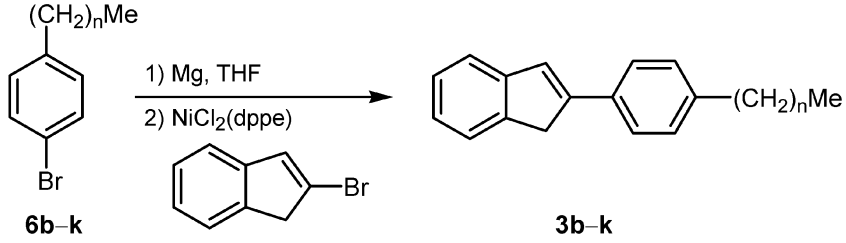


| 3, 6 | b | c | d | e | f | g | h | i | j | k |
|---|---|---|---|---|---|---|---|---|---|---|
| n | 0 | 1 | 2 | 3 | 4 | 5 | 6 | 7 | 8 | 9 |
| **3** Yield (%) | 37 | 52 | 52 | 62 | 80 | 59 | 72 | 68 | 86 | 45 |

Scheme 2. Preparation of target (alkylphenyl)indenes **3b–3k**.

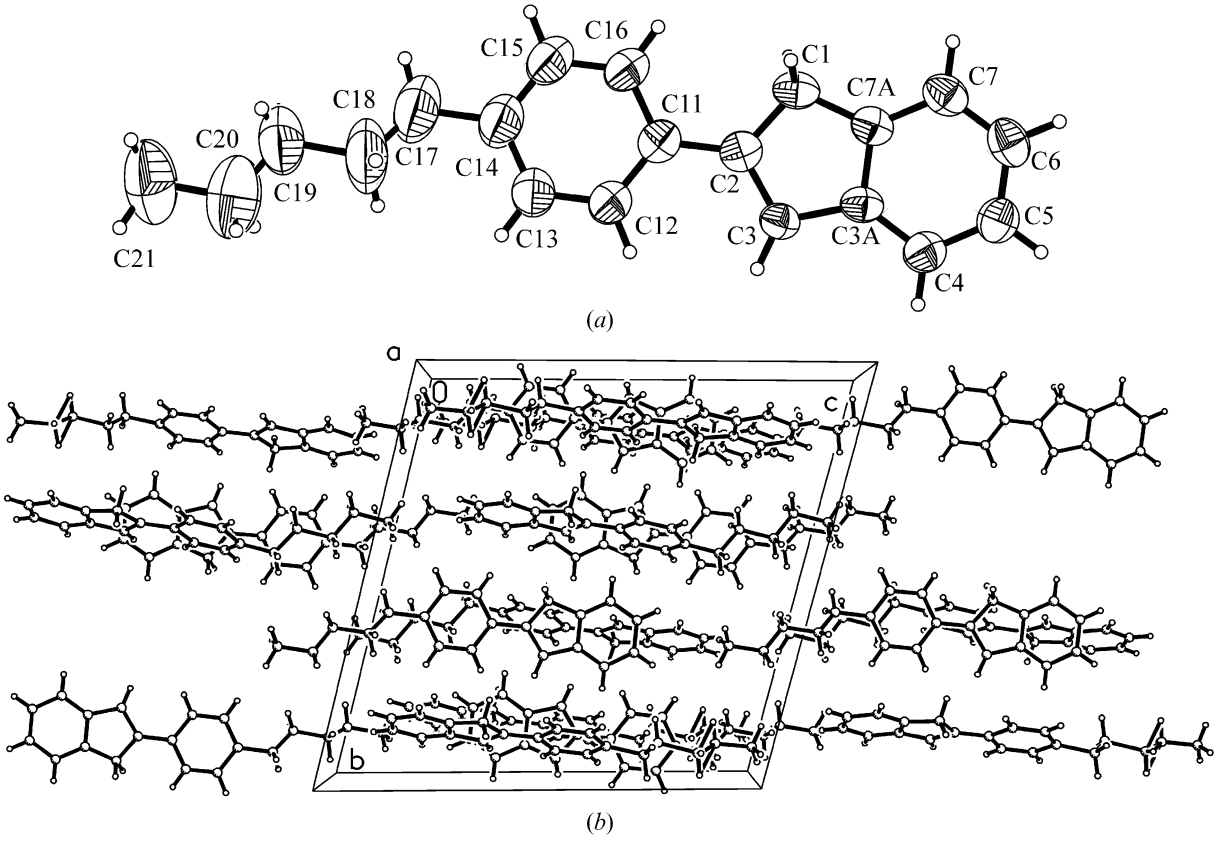


Figure 2. (a) Molecular structure of 2-(4-*n*-pentylphenyl)indene (**3f**) in the solid state and (b) a view of the ordered crystal packing of the molecules.

Table 1. Phase transition temperatures (°C) and enthalpies (kJ mol$^{-1}$, in brackets) of 2-phenylindene (**3a**) and 2-(4-*n*-alkylphenyl)indenes (**3b–3k**). The following phases were observed: $Cr_1$, $Cr_2$ (crystalline), CrE (crystal-smectic E), I (isotropic). (Phase observed, •; not observed, –; heating rate, 5 K min$^{-1}$).

| | Alkyl | $Cr_1$ | | $Cr_2$ | | CrE | | I | |
|---|---|---|---|---|---|---|---|---|---|
| **3a** | – | • | | – | | – | 167 (22.2) | • | 1. heating |
| **3a** | – | • | | – | | – | 155 (−20.4) | • | 1. cooling |
| **3b** | $CH_3$ | • | | – | | – | 174 (20.4) | • | 1. heating |
| **3b** | $CH_3$ | • | | – | | – | 171 (−16.8) | • | 1. cooling |
| **3c** | $C_2H_5$ | • | | – | | – | 169 (19.6) | • | 1. heating |
| **3c** | $C_2H_5$ | • | | – | | – | 166 (−19.0) | • | 1. cooling |
| **3d** | $C_3H_7$ | • | 130 (3.7) | – | | • | 152 (18.2) | • | 1. heating |
| **3d** | $C_3H_7$ | • | 110 (−3.1) | – | | • | 151 (−18.1) | • | 1. cooling |
| **3e** | $C_4H_9$ | • | 66 (3.6) | • | | – | 148 (17.6) | • | 1. heating |
| **3e** | $C_4H_9$ | – | | • | | – | 147 (−17.4) | • | 1. cooling |
| **3f** | $C_5H_{11}$ | • | 34 (2.7) | • | 83 (5.62) | • | 147 (17.8) | • | 1. heating |
| **3f** | $C_5H_{11}$ | • | 14 (−2.0) | – | | • | 148 (−18.6) | • | 1. cooling |
| **3g** | $C_6H_{13}$ | • | −32 (1.2) | – | | • | 142 (15.4) | • | 1. heating |
| **3g** | $C_6H_{13}$ | • | −26 (−2.2) | – | | • | 142 (−16.8) | • | 1. cooling |
| **3h** | $C_7H_{15}$ | • | 45 (5.9) | – | | • | 143 (18.3) | • | 1. heating |
| **3h** | $C_7H_{15}$ | • | 10 (−5.0) | – | | • | 142 (−18.2) | • | 1. cooling |
| **3i** | $C_8H_{17}$ | • | −32 (7.7) | • | 51 (13.7) | • | 141 (18.7) | • | 1. heating |
| **3i** | $C_8H_{17}$ | – | | • | −12 (−3.9) | • | 141 (−18.6) | • | 1. cooling |
| **3j** | $C_9H_{19}$ | • | 67 (13.1) | – | | • | 138 (18.3) | • | 1. heating |
| **3j** | $C_9H_{19}$ | • | 41 (−14.5) | – | | • | 138 (−18.2) | • | 1. cooling |
| **3k** | $C_{10}H_{21}$ | • | 35 (1.2) | • | 77 (17.3) | • | 136 (17.8) | • | 1. heating |
| **3k** | $C_{10}H_{21}$ | • | 45 (−1.3) | • | 55 (−18.3) | • | 134 (−18.0) | • | 1. cooling |

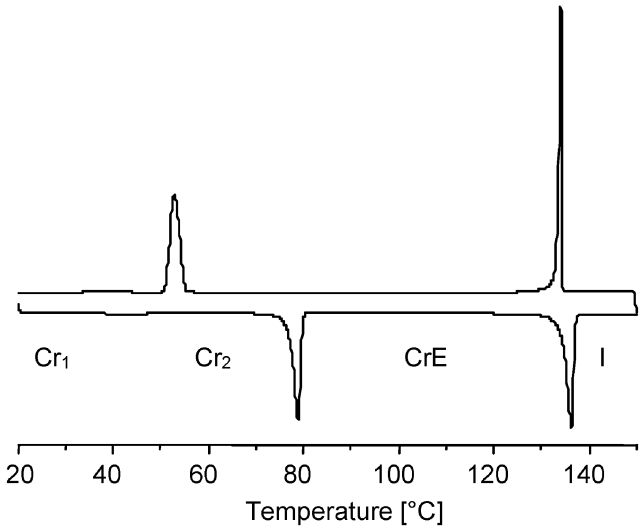


Figure 3. DSC curves (first heating and cooling cycle) of decyl derivative **3k** (heating rate 5 K min$^{-1}$). The following phases were observed: $Cr_1$, $Cr_2$ (crystalline), CrE (crystal-smectic E), I (isotropic).

The DSC results clearly indicate an additional enantiotropic phase between the isotropic melt and the crystalline state of the decyl homologue **3k** (figure 3). The possibly liquid-crystalline nature of this mesophase was carefully investigated by POM and X-ray scattering. Textures of **3k**, as observed between crossed polarizers, are depicted in figure 4. Below 134°C (figure 4a) the optically isotropic melt transformed into a spontaneously birefringent fluid, the fluidity of which was proven by mechanically shearing the sample between the cover slip and the slide. The combination of fluidity and optical anisotropy gives clear evidence of a liquid crystalline state. The phase boundary in figure 4a further confirmed a dendritic growth of the liquid crystalline phase from the isotropic melt. After completion of the phase transition (figure 4b), the mesophase of **3k** developed a characteristic texture, which is known as 'platelet texture'.

Both the platelet texture and its dendritic growth are typical for the formation of a higher-ordered crystal-smectic E phase [6, 13]. Upon cooling from the isotropic phase platelets developed rapidly. During growing the platelets overlapped one another so that the typical ''ghost-like'' images of platelets are seen through upper platelets [6]. This texture is known to be unique to the crystal-smectic E phase [14].

X-ray diffraction turned out to be the most powerful tool in the experimental study of the smectic structures [15]. Selected examples of the X-ray diffraction profiles obtained for the derivatives **3h–3k** are shown in figure 5.

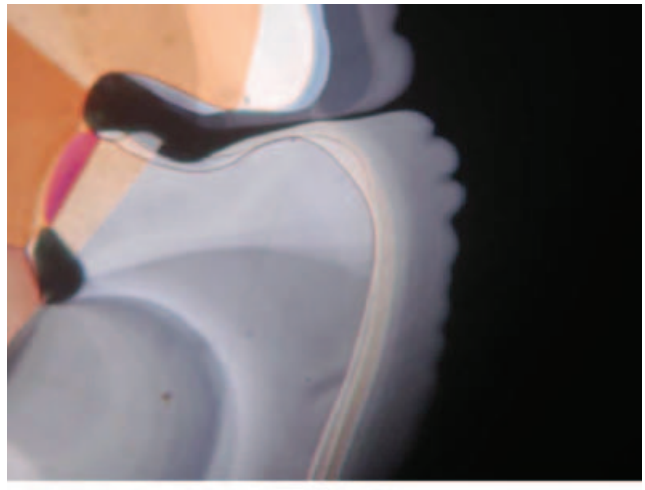

(*a*)

(*b*)

Figure 4. Mesophase textures of the decyl homologue **3k** observed in the polarizing microscope. (a) Dendritic growth of the crystal-smectic phase from the isotropic melt (black) at 134°C; (b) fully-developed platelet texture of the crystal-smectic E phase at 120°C (magnification 200×).

The scattering profiles obtained from the liquid-crystalline phases at 120°C each show four distinct scattering peaks. Whereas the smectic layer peak observed in the small-angle regime varies according to the length of the molecules **3h–3k**, the three wide-angle peaks, indicating the intralayer order, remain essentially unchanged (figure 6). Thus, the smectic phases of **3h–3k** have the same intralayer order.

In each case the smectic layer spacing $d$ ($d$=26 Å for **3k**) compares or slightly exceeds the length $L$ ($L$=23 Å for **3k**) of a fully extended molecule (figure 7a) and therefore, only non-tilted smectic structures like SmA, SmE or SmB are taken into account. The quite narrow wide-angle peaks (figure 6) indicate long-range in-plane order of the mesogens and clearly exclude fluid layers

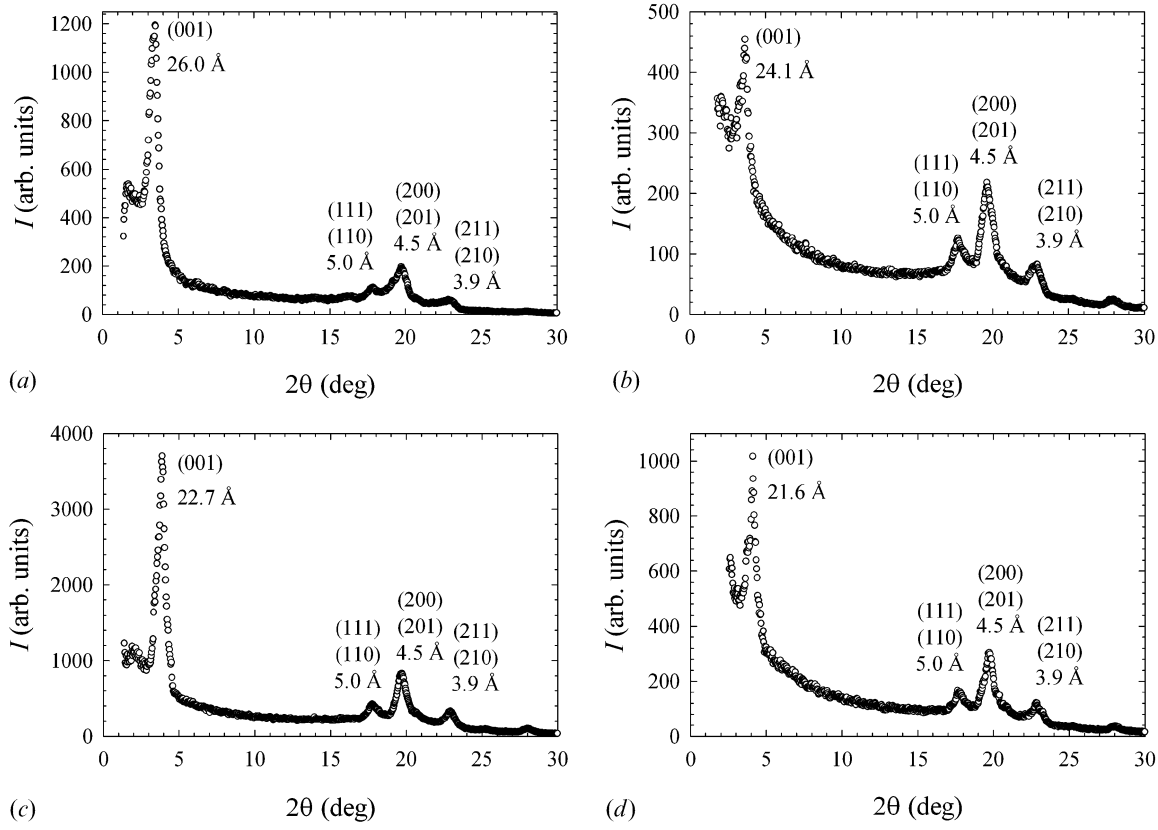


Figure 5. X-ray diffraction profiles of the homologues **3k** (a), **3j** (b), **3i** (c), and **3h** (d) in the crystal-smectic E phase at 120°C.

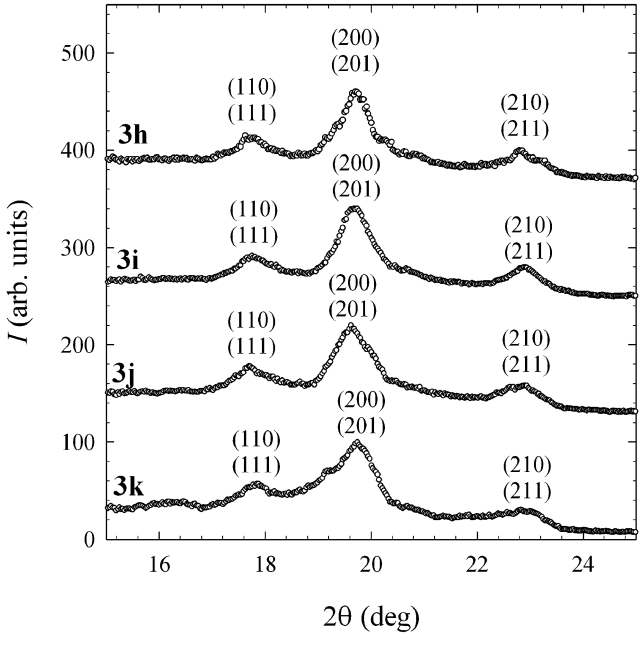


Figure 6. X-ray diffraction profiles in the wide-angle regime of the homologues **3k**, **3j**, **3i** and **3h** in the crystal-smectic E phase at 120°C.

typical for SmA and SmC phases [13]. The SmB phase is excluded due to the fact that three reflections instead of one were observed. Instead, the three wide-angle peaks conform to an E phase, showing at least three narrow wide-angle peaks [15]. In addition, the existence of E phases in **3h–3k** is fully in line with the characteristic 'platelet texture' observed in the polarizing microscope (see figure 4). Consequently, the wide-angle peaks shown in figure 6 were indexed according to the orthorhombic structure of an E phase (figure 7b) [6].

The observed and calculated scattering angles of derivative **3k** with its corresponding lattice constants *a*, *b*, *c* are summarized in table 2. The *a*:*b* ratio is in good agreement with the results for the CrE phase of compound **1** (scheme 1), and, similar to our findings, Leadbetter also reported the layer spacing of the E phase to be slightly higher than the molecular length [2b].

In conclusion, the non-conventional mesogens, 2-(4-*n*-alkylphenyl)indenes (**3d**, **3f–3k**), bearing only one lateral alkyl chain at the rigid core, display higher-ordered smectic mesophases. In the case of **3k**, both POM and X-ray diffraction studies consistently confirm the existence of the rare higher-ordered crystal-smectic

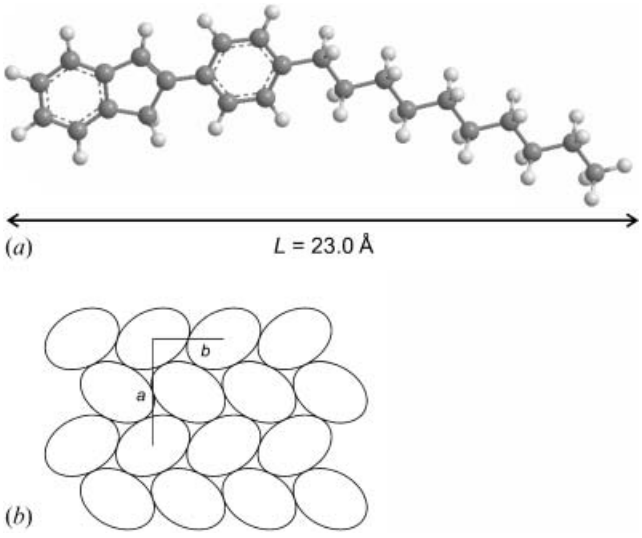


Figure 7. (a) Conformation of the molecule **3k** after energy minimization using MOPAC/AM1. (b) Herringbone packing of the molecules in the crystal-smectic E phase (after Gray and Goodby [6]).

E phase between the isotropic and the crystalline state. Keeping in mind that compounds **3** were originally intended as ligands for metallocenes, their mesomorphic properties might give access to novel metallomesogens. Even if the metallocene itself is non-mesomorphic, miscibility with an ordered mesophase-containing ligand should lead to mesophase-assisted Ziegler–Natta polymerization. Thus, promising stereoselectivities of the growing polymer due to the mesophase template might be expected.



**Acknowledgements**

This work was generously supported by the Deutsche Forschungsgemeinschaft, the Fonds der Chemischen Industrie and the Ministerium für Wissenschaft, Forschung und Kunst des Landes Baden-Württemberg.

Table 2. Observed and calculated *d* values of compound **3k** indexed according to the orthorhombic E phase.

| $2\theta_{calcd}$ | $2\theta_{obs}$ | $d_{obs}$ /Å | *h k l* | Lattice constants /Å |
|---|---|---|---|---|
| 3.40 | 3.40 | 26.02 | 001 | $a$=9.28 |
| 17.1 | 17.8 | 4.97 | 110 | $b$=6.24 |
| 17.5 | | | 111 | $c$=26.02 |
| 19.1 | 19.7 | 4.50 | 200 | |
| 19.4 | | | 201 | |
| 23.9 | 22.9 | 3.88 | 210 | |
| 24.1 | | | 211 | |

**References**

[1] P.G. de Gennes, J. Prost. *The Physics of Liquid Crystals*; second edn, Oxford Science Publications, Clarendon Press, Oxford (1993).

[2] (a) G.W. Gray, K.J. Harrison. *Mol. Cryst. liq. Cryst.*, **13**, 37 (1971); (b) A.J. Leadbetter, M.A. Mazid, K.M.A. Malik. *Mol. Cryst. liq. Cryst.*, **61**, 39 (1980).

[3] S. Ito, M. Ando, A. Nomura, N. Morita, C. Kabuto, H. Mukai, K. Ohta, J. Kawakami, A. Yoshizawa, A. Tajiri. *J. Org. Chem.*, **70**, 3939 (2005).

[4] R. Eidenschink (Merck Patent GmbH). Ger. Offen. DE 4 303 634 (1994) [*Chem. Abstr.*,**122**, 68445 (1995)].

[5] (a) G.W. Coates, R.M. Waymouth. *Science*, **267**, 247 (1995); (b) S. Lin, R.M. Waymouth. *Accts Chem. Res.*, **35**, 765 (2002).

[6] G.W. Gray, J.W. Goodby. *Smectic Liquid Crystals – Textures and Structures*, pp. 82–93, Leonhard Hill, Glasgow (1984).

[7] (a) L.G. Greifenstein, J.B. Lambert, R.J. Nienhuis, H.E. Fried, G.A. Pagani. *J. Org. Chem.*, **46**, 5125 (1981); (b) I.E. Nifant'ev, A.A. Sitnikov, N.V. Andriukhova, I.P. Laishevtsev, Y.N. Luzikov. *Tetrahedron Lett.*, **43**, 3213 (2002).

[8] (a) W. Zhu, C. Liu, L. Su, W. Yang, M. Yuan, Y. Cao. *J. Mater. Chem.*, **13**, 50 (2003); (b) M.R. Friedman, K.J. Toyne, J.W. Goodby, M. Hird. *Liq. Cryst.*, **28**, 901 (2001); (c) G.W. Gray, M. Hird, D. Lacey, K.J. Toyne. *J. Chem. Soc., Perkin Trans. 2*, 2041 (1989); (d) S. Franks, F.R. Hartley. *J. Chem. Soc., Perkin Trans. 1*, 2233 (1980).

[9] Adapted from the procedure in: T. Soós, B.L. Bennett, D. Rutherford, L.P. Barthel-Rosa, J.A. Gladysz. *Organometallics*, **20**, 3079 (2001).

[10] (a) K. Tamao, K. Sumitani, M. Kumada. *J. Am. chem. Soc.*, **94**, 4374 (1972); (b) R.J. Corriu, J.P. Masse. *Chem. Commun.*, 144 (1972); (c) K. Tamao, K. Sumitani, Y. Kiso, M. Zembayashi, A. Fujioka, S. Kodama, I. Nakajima, A. Minato, M. Kumada. *Bull. chem. Soc. Japan,* **49**, 1958 (1976); (d) M. Kumada. *Pure appl. Chem.*, **52**, 669 (1980); (e) reviewed by V.N. Kalinin. *Synthesis*, 413 (1992).

[11] (a) R.L. Halterman, D.R. Fahey, E.F. Bailly, D.W. Dockter, O. Stenzel, J.L. Shipman, M.A. Khan, S. Dechert, H. Schumann. *Organometallics*, **19**, 5464 (2000); (b) I. McEwen, M. Rönnquist, P. Ahlberg. *J. Am. chem. Soc.*, **115**, 3989 (1993); (c) D.R. Dalton, V.P. Dutta, D.C. Jones. *J. Am. chem. Soc.*, **90**, 5498 (1968).

[12] Single crystals of **3f** were obtained from a concentrated heptane solution at room temperature. Formula $C_{20}H_{22}$, M=262.38, colourless crystal $0.25 \times 0.20 \times 0.03$ mm, triclinic, space group P1bar (No. 2), a=9.291(1), b=18.725(1), c=18.855(1) Å, $\alpha$=103.50(1), $\beta$=93.18(1), $\gamma$=99.49(1)°, V=3130.9(4) $Å_3$, $\rho_{calc}$=1.113 g $cm_{-3}$, Z=8, empirical absorption correction ($0.893 \leqslant T \leqslant 0.986$), CuK$\alpha$ radiation, $\lambda$=1.54178 Å, T=223 K, $\omega$ and $\varphi$ scans, 35 206 reflections collected ($\pm$h, $\pm$k, $\pm$l), [$(\sin\theta)/\lambda$]=0.58 $Å_{-1}$, 9752 independent (Rint=0.106) and 5808 observed reflections [$I \geqslant 2\ \sigma(I)$], 725 refined parameters, $\mu$=0.463 $mm_{-1}$, R=0.088, wR2=0.258, max. residual electron density 0.31 (−0.25) e $Å_{-3}$, hydrogen atoms calculated and refined as riding atoms, crystals of poor quality leads to an analysis of limited accuracy. The data set was collected with a Nonius KappaCCD

diffractometer. Programs used: data collection COLLECT (Nonius BV, 1998); data reduction Denzo-SMN [Z. Otwinowski, W. Minor. *Meth. Enzymol.*, **276**, 307 (1997)]; absorption correction Denzo [Z. Otwinowski, D. Borek, W. Majewski, W. Minor. *Acta crystallogr. A*, **59**, 228 (2003)]; structure solution SHELXS-97 [G.M. Sheldrick. *Acta crystallogr. A*, **46**, 467 (1990)]; structure refinement SHELXL-97 [G.M. Sheldrick. Universität Göttingen (1997)]; graphics SCHAKAL [E. Keller. Universität Freiburg (1997)]. CCDC-283145 contains the supplementary crystallographic data for this paper that can be obtained free of charge from the Cambridge Crystallographic Data Centre via www.ccdc.cam.ac.uk/data_request/cif.

[13] D. Demus, L. Richter. *Textures of Liquid Crystals,* Deutscher Verlag für Grundstoffindustrie, Leipzig (1978); see, for example, plate 133.

[14] As stated by Goodby, the E phase exhibits a platelet texture, which often appears grey-blue to yellowish in colour. The texture is very different to normal mosaic textures in that the transparent platelets overlap so that ghost-like images of platelets can be seen through platelets near to the surface. This type of texture is unique to the E phase and therefore makes it readily identifiable (see ref. [6], p. 91).

[15] J.M. Seddon. In *Handbook of Liquid Crystals,* Vol. 1, D. Demus, J.W. Goodby, J.W. Gray, H.-W. Spiess, V. Vill (Eds), pp. 635–679, Wiley-VCH, Weinheim (1998).